Modified Angelov model for an exploratory GaN-HEMT technology with short, few-fingered gates

Sumit Emekar*, Jaya Jha†, S. Mukherjee, M. Meer, K. Takhar, D. Saha, S. Ganguly‡
Department of Electrical Engineering
Indian Institute of Technology, Bombay
Mumbai, India
Email: *sumitemekar@ee.iitb.ac.in, †jayajha@ee.iitb.ac.in, ‡sganguly@ee.iitb.ac.in

***Abstract*— The GaN-based HEMT has emerged as a leading technology option for high-power and high-frequency applications because of its outstanding electronic properties. Angelov-GaN is one of the most popular compact models for GaN-HEMT devices. However, we observed that the standard Angelov-GaN model is unable to accurately model small gate length and gate width HEMT. In this work, we present a modified version of the Angelov-GaN model that captures dc and ac non-idealities in exploratory technology HEMTs. In order to capture these effects we extend the standard DC model using parametric analysis; for RF modeling, we use the open-short de-embedding technique to capture additional pad parasitic effects. The modelled DC I-V and bias dependent S-parameters are found to be in good agreement with measured experimental data.**

***Keywords*— AlGaN/GaN HEMT, Compact Modeling, De-embedding**

I. INTRODUCTION

The GaN high-electron mobility transistor (HEMT), using the two-dimensional electron gas (2DEG) at the AlGaN/GaN hetero-interface, has established itself as the device of choice for many high speed and high power applications [1]. Naturally, device compact models need to be available in computer-aided design (CAD) tools for the design and simulation of GaN-HEMT based radio-frequency (RF) circuits like LNA, mixers, and oscillators. 'Angelov-GaN' is a popular semi-empirical compact model for GaN-HEMTs [2]. In this work, we have extended the standard Angelov-GaN model to an exploratory technology wherein the gate region is selectively wet-recessed and then wet-oxidized to give a thin Al_2O_3 layer (refer Fig. 1), leading to improved DC and RF performance [3]. Figure 1 shows typical thickness of each material layer in the heterostructure along with band bending at the hetero-interface and 2DEG. The heterostructure used in this study is grown by metal organic chemical vapor deposition (MOCVD) on a SiC substrate. The unintentionally n-doped AlGaN barrier is composed of 30% Al. The 2-DEG density and mobility are found to be 8.7×10^{12} cm^{-2} and 2200 $cm^2V^{-1}s^{-1}$, respectively using Hall measurement. The source/drain contacts are Ti/Al/Ni/Au (30/130/30/300 nm). The AlGaN barrier is first recess-etched by 2 ± 0.8 nm. Then the sample is treated with 30% H_2O_2 solution to grow 4.2 ± 1.2 nm of Al_2O_3. Finally, Ni/Au (30/300 nm) gate contacts are defined by lift-off [3-4]. DC and RF characterization were performed using source meter (Keithley 2602A), network analyzer (PNA-X 5244A) and RF probing station with standard GSG probes. The fabricated device pads are defined in the GSG configuration. From Fig. 1, L_G indicates gate length where as L_{SG} and L_{DG} are the source-to-gate and gate-to-drain access region. The quality of the gate Schottky contact decides gate leakage current and quality of source/drain ohmic contacts decides contact resistance, which controls the drain current in channel. We note that the devices are short-channel (L_G = 580nm) and, in keeping with the exploratory nature of the technology, have 2 gate fingers. We find that the former introduces a bias-dependent non-linearity, while the later introduces additional pad parasitics in this exploratory HEMTs, neither of which are included in the standard Angelov-GaN model.

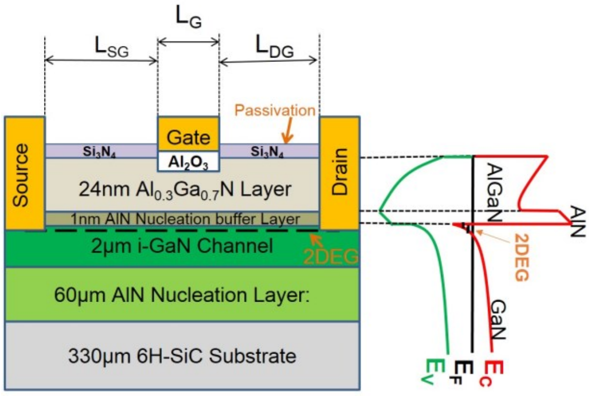

Fig. 1: HEMT structure

II. MODEL AND EXTRACTION

The Angelov model [5], developed from the Curtice FET model [6], captures GaN specific effects, e.g. formulation of gate-leakage current, electro-thermal model for self-heating effect, input output dispersion effect at high frequencies, capacitance peaking [2, 5, 7-8]. In this work the Angelov GaN model is extended to capture additional pad parasitics and bias dependent non-linearity in an exploratory GaN HEMT technology.

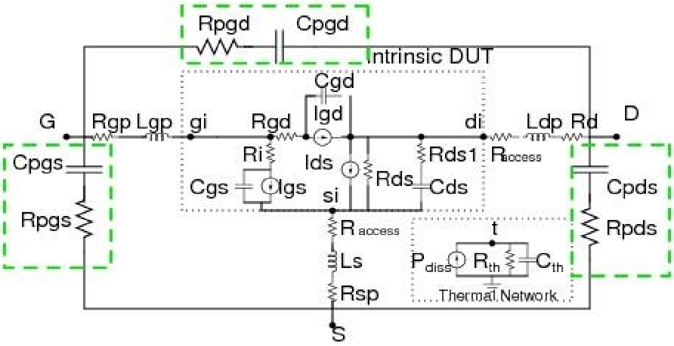

Fig. 2: Modified equivalent circuit

A. *Extended Angelov GaN Model*

The equivalent circuit for the modified Angelov GaN model is shown in Fig. 2 with highlighted modifications in pad parasitics. The current source I_{DS} gives DC drain current. The gate capacitances C_{gs} and C_{gd}, gate Schottky diode elements R_i, R_{gd} and output elements C_{ds1} and R_{ds1} model high frequency effects. The current sources I_{gs} and I_{gd} model gate diode leakage currents. The circuit elements P_{diss}, R_{th}, C_{th} comprise the thermal model to capture self-heating effect. Equations 1-4 describe basic Angelov Gan model used in this work for further development [5].

$$I_{DS} = I_{pk0}(1+\tanh(\psi))(1+\lambda.V_{DS})\tanh(\alpha.V_{DS}) \tag{1}$$

$$\psi = \sinh\left(\left[1+\frac{B_1}{\cosh^2(B_2.V_{DS})}\right](P_1\,(V_{GS}-V_{pk})+P_2(V_{GS}-V_{pk})^2+P_3(V_{GS}-V_{pk})^3)\right) \tag{2}$$

$$V_{pk}(V_{DS}) = V_{pk0}+(V_{pks}-V_{pk0})\tanh(\alpha.V_{DS}) \tag{3}$$

$$\alpha = \alpha_r + \alpha_s[1+\tanh(\psi)] \tag{4}$$

where, I_{pk0} and V_{pk} is drain current and gate voltage at maximum g_m,

ψ is power series centered at V_{pk} with variable V_{GS}, decides shape of g_m,

α is saturation parameter, λ is channel length modulation parameter,

B_1, B_2, P_1, P_2, P_3 are fitting parameters.

The parameter P_1 defines transconductance g_m at $V_{gs} = V_{pk}$. The coefficient P_2 in power series ψ makes g_m asymmetric and P_3 affects drain current at V_{gs} near to pinch off voltage. In order to achieve high accuracy at lower drain bias, it is essential to add drain bias dependency in parameters P_1 and V_{pk} [7]. Weak dependence of V_{pk} on drain voltage V_{ds} observed in HEMTs is captured in the Equation 3. For large drain and gate voltage variations, the saturation parameter α cannot be assumed constant [7]. The drain and gate bias dependency for parameter α is being captured in Equation 4.

The advantage of this model is simplicity in extracting the model parameters. The parameter λ is extracted from the slope of I_{ds}–V_{ds} characteristics at saturated channel conditions. I_{pk} and V_{pk} can be extracted from $g_m - V_{gs}$ curve at maximum transconductance g_{mpk}. Coefficients $P_{i=1,2,3}$ can be extracted by fitting experimental data. The intrinsic circuit and parasitic elements are being extracted from experimental S-parameter data. Generic extraction functions are implemented in ICCAP Angelov GaN modeling package. The extraction procedure is modified according to present available characterization lab facility and to be suitable for improvements in Angelov GaN model to capture transconductance dependency at low drain bias, extra pad parasitics for these exploratory technology HEMT devices.

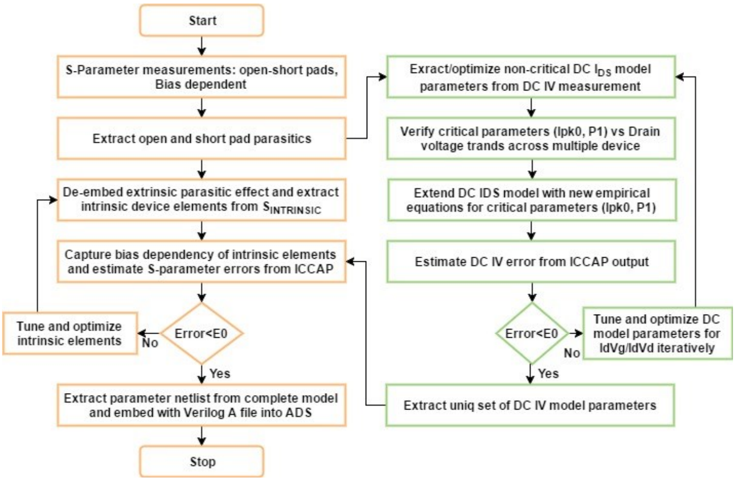

Fig. 3: Detailed modeling methodology (RF and DC)

III. METHODOLOGY

We propose here a simplified methodology for parametric analysis to extend the Angelov-GaN model with new empirical equations to capture drain voltage dependent non-linearity in DC model. It was seen that for these devices with small effective gate width (i.e. 1-2 gate fingers), de-embedding with the standard Angelov-GaN equivalent circuit is insufficient – possibly due to 'crosstalk' between the source/drain pads which are not well-separated by the gate. The modifications done to capture these parasitic effects for more accurate de-embedding are highlighted in Fig. 2. The ohmic contact resistance (R_{ohmic}), access region resistance (R_{access}) are considered to be bias independent and their bias dependency is captured in dependent current source I_{DS} which constitute the DC model. The model extraction methodology used for DC and RF modeling is summarized in Fig. 3.

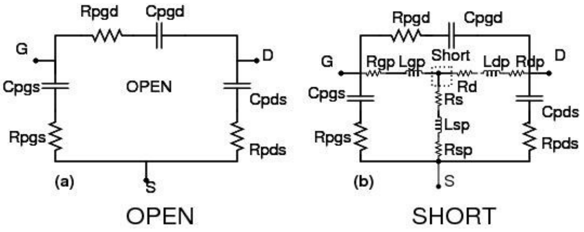

Fig. 4: Equivalent circuit of (a) Open pad (b) Short Pad

A. *Pad parasitics extraction*

After DC and RF characterization the first step is to extract extrinsic pad parasitics from open and short pad S-parameter. During device fabrication, open and short pad structures are also prepared on the same sample with devices for de-embedding purpose. These have same dimensions as of actual device pads. Equivalent circuit for Open and Short pads are shown in Fig. 4(a, b) respectively.

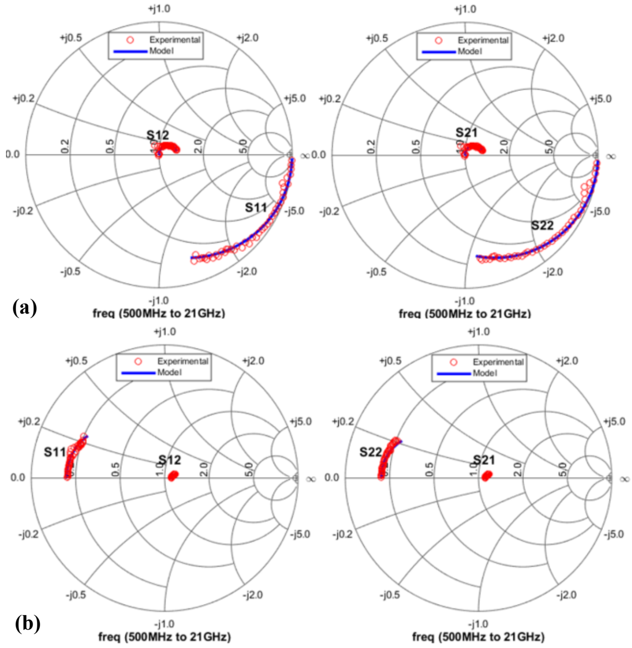

Fig. 5: S-parameter modelling results for (a) open (b) short pad

S-parameters for open pad are used to extract R_{pgs}, R_{pgd}, R_{pds}, C_{pgs}, C_{pgd}, C_{pds} by comparing standard π-network with its equivalent circuit. Whereas, Y-parameter difference between short and open pad yields de-embedded short pad T-network to extract R_{gp}, R_{dp}, R_{sp}, L_{gp}, L_{dp}, L_{sp}. Since experimental S-parameter data has irregularities present over the frequency range, we cannot extract values of these passive elements at single frequency point. Hence, lumped element values are averaged over frequency range 10GHz to 20GHz. Modeling results for open and short pads are shown in Fig. 5(a, b), indicating extended equivalent circuit model for open and short pads is in good agreement with experimental data.

B. Bias dependent parametric analysis

After pad parasitic extraction, DC model parameters λ, α_s, α_r, R_{th}, I_{pk0}, P_1, P_2, P_3, B_1, B_2, V_{pks}, DV_{pks}, combination of ohmic contact resistance and access region resistance on source and drain side are extracted, based on DC IV experimental data using ICCAP extraction and optimization routine followed by manually tuning of parameters to its best fit. Although this procedure of optimization and tuning gives close fit, but still fitting results are not found in acceptable RMS error range. It is observed that the present Angelov GaN HEMT model in ICCAP requires additional analytical functions to capture non-linearity to give unique parameter set for complete experimental data set. It has been observed from $g_m - V_{GS}$ experimental data (as in Fig. 6), shift in peak of g_m varies more with drain voltage as compared to the default model in [2]. For better accuracy in fitting experimental data, transconductance g_m vs V_{GS} need to be modeled well [5]. In order to model asymmetry and shift observed in g_m peak in our devices, which arises possibly from short-channel effects, a bias-dependent parametric analysis method is applied with introducing new empirical equations in terms of critical parameters I_{pk0} and P_1.

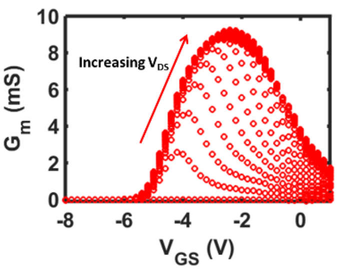

Fig. 6: Observed drain dependent g_{mMAX} shift from experimental data

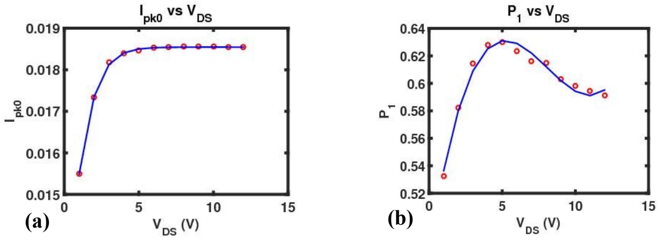

Fig. 7: Modeling variation of (a) I_{pk0} (b) P_1

In this method, the DC model parameters are initially extracted to their first guess values from the experimental I-V data. Individual $I_D - V_G$ fitting at different drain bias is then carried out by optimizing the critical parameters I_{pk0}, P_1, P_2, and P_3. In order to confirm the drain voltage non-linearity, critical parameter versus drain voltage (V_{DS}) curves being plotted across multiple devices. This drain voltage dependency is then captured with introducing new analytical equation for one parameter at a time according to observed sensitivity from the plot. First I_{pk0} versus V_{DS} is modelled using Equation 5 with two new fitting parameters. It has been taken care to have least number of fitting parameter with minimum analytical equations in overall extended model. Again similar procedure of individual I_D–V_G fitting across different V_{DS} is carried out, with optimizing only P_1. It is observed that with new analytical function for I_{pk0} in place, parameter P_1 is sufficient to reduce RMS error within acceptable range for $g_m - V_{GS}$ curve. The observed drain voltage dependency in P_1 is captured by introducing second analytical fitting function as in Equation 6. Figure 7 shows the fitting results for I_{pk0} and P_1 versus drain voltage using Equations 5-6. This extended model is implemented in Verilog A and verified for accuracy using the ICCAP device modeling software. Finally, a unique set of DC model parameters is extracted and used for RF modeling.

$$I'_{pk0} = I_{pk0}(\tanh(S_1.V_{DS}) + S_2) \qquad (5)$$

$$P'_1 = P_1.V_{DS}^3 + S_3.V_{DS}^2 + S_4.V_{DS} + S_5 \qquad (6)$$

where, $S_{1..4}$ are new fitting parameters.

The results obtained for DC I-V extended model are shown in Fig. 8. The fitting performance is measured in terms of coefficient of determination (R^2) and root mean square (RMS) value. Values of R^2 and RMS error for this fitting are 99.97% and 0.19mA respectively, over the drain current range of 0-40mA, implying near-complete agreement with DC I-V experimental data.

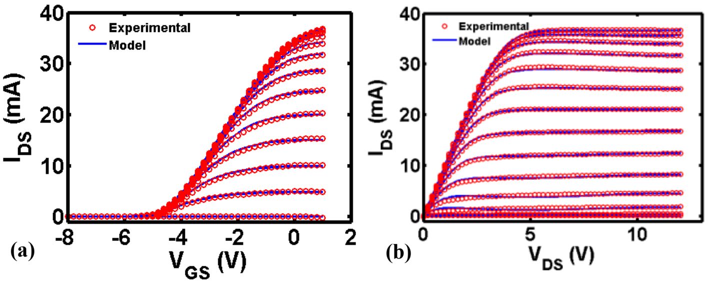

Fig. 8: Experimental and modelled DC (a) I_{DS}-V_{GS} (b) I_{DS}-V_{DS}

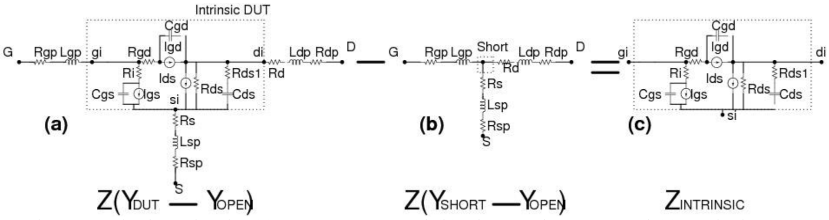

Fig. 9: Equivalent circuits (a) DUT – Open pad (b) Short pad – Open pad (c) Intrinsic DUT

C. RF Modeling

While studying the high frequency performance of GaN HEMTs, it is important to model bias dependent intrinsic device elements present in small signal equivalent circuit. Accuracy of small signal model is vital for designing RF circuits. Bias dependent S-parameters were measured over frequency range of 0.5 to 21 GHz. The de-embedding is essential to remove effect of external parasitic elements for extracting intrinsic device elements.

Open-short de-embedding method

Open-short de-embedding method is used for subtracting the effect of pads from bias dependent S-parameter data of device under test (DUT) [9]. For accurate de-embedding, open-short test structures fabricated on the same wafer with same dimensions as that of the pads used for DUT. The simulated data of equivalent circuit for open and short pads extracted in earlier step, is used here to reduce errors due to irregularities in experimental data. From Fig. 2, we note that the equivalent circuit for the open pad appears in parallel with the equivalent circuit of short pad as well as the DUT. Hence open pad parasitic effect can be removed from DUT and short pads by subtraction of corresponding Y-parameters, as shown with resultant equivalent circuit in Fig. 9 (a) and (b) respectively. The difference between the Z-parameters of these two networks yields Z-parameters of intrinsic device (Fig. 9 (c)) which are converted into $S_{Intrinsic}$ as expressed in Equations 7-8.

$$Z_{INTRINSIC} = Z(Y_{DUT} - Y_{OPEN}) - Z(Y_{SHORT} - Y_{OPEN}) \quad (7)$$

$$S_{INTRINSIC} = S(Z_{INTRINSIC}) \quad (8)$$

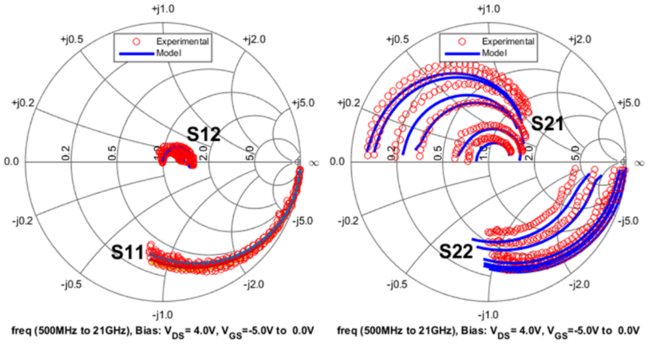

Fig. 10: Gate bias dependent S-parameter at V_{DS}= 4V (const.)

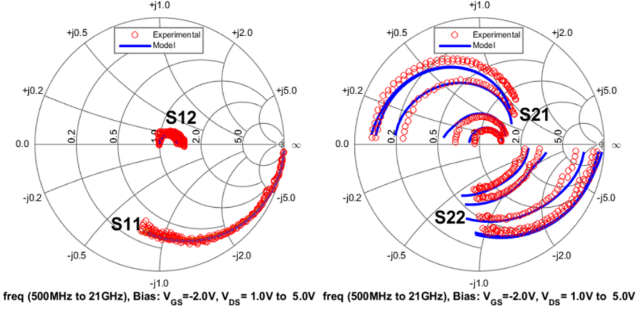

Fig. 11: Drain bias dependent S-parameter at V_{GS}= -2V (const.)

Intrinsic device circuit elements are then extracted from $S_{Intrinsic}$ using equations derived from network synthesis. Since the experimental S-parameter data has irregularities present over the frequency range, lumped element values are averaged over frequency range of 10GHz to 20GHz and are further manually tuned for better fitting of individual S-parameters. The complete model in Verilog A and parameter netlist is embedded into Agilent's ADS circuit simulator for validation. The fitting results for the RF S-parameters within the bias range (V_{GS}=-5V to 0V; V_{DS}=1V to 5V) and frequency range (500MHz to 21GHz) are shown in Fig. 10-11, indicating good agreement.

IV. CONCLUSION

We demonstrate a methodology to adapt the Angelov-GaN model for GaN-HEMT technologies comprising small gate length and (effective) width. It involves modification of the DC current equations, and of the pad parasitics for AC.

ACKNOWLEDGMENT

The authors would like to acknowledge support from the Ministry of Electronics and Information Technology, Government of India, through the Centre of Excellence in Nanoelectronics at IIT Bombay.

REFERENCES

[1] U. K. Mishra, P. Parikh and Y.-F. Wu, "AlGaN/GaN HEMTs-an overview of device operation and application," in Proceedings of the IEEE, vol. 90, no. 6, pp. 1022–1031, Jun 2002.

[2] I. Angelov, M. Thorsell, K. Andersson, A. Inoue, K. Yamanaka, and N. Hifumi, "On the large signal evaluation and modeling of gan fet," IEICE transactions on electronics, vol. 93, no. 8, pp. 1225–1233, 2010.

[3] K. Takhar, M. Meer, B. B. Upadhyay, S. Ganguly and D. Saha, "Performance improvement and better scalability of wet-recessed and wet-oxidized AlGaN/GaN high electron mobility transistors," in Solid-State Electronics 131C, (39-44), May 2017.

[4] M. Mudassar, M. Sridhar T Kuldeep, S Ganguly, D Saha, "Impact of Wet-oxidized Al2O3/AlGaN Interface on AlGaN/GaN 2-DEGs", Semiconductor Science and Technology 32, 04LT02 (2017).

[5] I. Angelov, H. Zirath, and N. Rosman, "A new empirical nonlinear model for HEMT and MESFET devices," Microwave Theory and Techniques, IEEE Transactions on, vol. 40, pp. 2258–2266, 1992.

[6] W. R. Curtice and M. Ettenberg, "A nonlinear GaAs FET model for use in the design of output circuits for power amplifiers," IEEE Transactions on Microwave Theory Techniques, vol. 33, pp. 1383–1394, 1985.

[7] I. Angelov, L. Bengtsson, and M. Garcia, "Extensions of the chalmers nonlinear hemt and mesfet model," Microwave Theory and Techniques, IEEE Transactions on, vol. 44, no. 10, pp. 1664–1674, 1996.

[8] I. Angelov, K. Andersson, D. Schreuers, N. Rorsman, V. Desmaris, M. Sudow, and H. Zirath, "Large-signal modeling and comparison of algan/gan hemts and sic mesfets," GaN, vol. 1, p. 2, 2006.

[9] J. W. Chung, "Millimeter-wave GaN high electron mobility transistors and their integration with silicon electronics," PhD diss., Massachusetts Institute of Technology, 2011.